



# **Non-linear Regression, a Better Approach for the Optimisation of Hydroquinone, Resorcinol and Catechol Adsorption by Chemically Activated Carbon Based on Monkey Kola (*Cola lepidota* k. schum) Waste**

**Nono Nguemjom Patricia<sup>1,2</sup>, Kamgaing Théophile<sup>1\*</sup>,  
Tchuifon Tchuifon Donald Raoul<sup>1</sup>, Doungmo Giscard<sup>1</sup>,  
Baleba Mbanga Moise Roger<sup>2</sup> and Anagho Solomon Gabche<sup>1,3</sup>**

<sup>1</sup>*Research Unit of Noxious Chemistry and Environmental Engineering, Department of Chemistry, Faculty of Science, University of Dschang, P.O Box, 67. Dschang, Cameroon.*

<sup>2</sup>*Laboratory for food study and quality control, Centre for Food and Nutrition Research, Institute of Medical Research and Medicinal Plants Studies, Ministry of Scientific Research and Innovation, P.O Box, 13033, Yaounde, Cameroon.*

<sup>3</sup>*Department of Chemistry, University of Bamenda, P.O Box 39, Bamenda, Cameroon.*

## **Authors' contributions**

*This work was carried out in collaboration between all authors. All authors read and approved the final manuscript.*

## **Article Information**

DOI: 10.9734/CSJI/2018/45320

### Editor(s):

(1) Dr. Nagatoshi Nishiwaki, Professor, Kochi University of Technology, Japan.

### Reviewers:

(1) Victor Shikuku, Kaimosi Friends University College, Kenya.

(2) Farid I. El-Dossoki, Port Said University, Egypt.

Complete Peer review History: <http://www.sciencedomain.org/review-history/27684>

**Original Research Article**

**Received 21 September 2018**

**Accepted 27 November 2018**

**Published 08 December 2018**

## **ABSTRACT**

Activated carbon was prepared from waste of monkey kola by pyrolysis and chemical activation using  $H_3PO_4$ . It was characterised by Fourier transform infrared spectroscopy (FTIR), X-ray diffraction (XRD) and energy dispersive X-ray spectroscopy (EDX). Different physical properties namely bulk density, moisture content, volatile matter content, iodine number, pH of the solution, pHpzc and methylene blue adsorption were also determined. The activated carbon was used as an

\*Corresponding author: E-mail: [theokamgaing@yahoo.fr](mailto:theokamgaing@yahoo.fr);

adsorbent for the removal of hydroquinone, catechol and resorcinol in solution. The process parameters of the sorption system such as pH of the solution, contact time and the amount of adsorbent were studied to understand their effects on pollutants removal. The optimised parameters are found to be pH: between 6 - 8, and the agitation time: 30 minutes. The experimental equilibrium data were analysed using five models (Langmuir, Freundlich, Redlich-Peterson, Sips, Langmuir-Freundlich). Non-linear regression analysis was employed, and three error analysis methods, correlation coefficient ( $R^2$ ), root-mean-square error (RMSE) and non-linear chi-square test ( $\chi^2$ ) were considered to identify the best-fit isotherm and the best-fit kinetic model. Among all the adsorption isotherms considered, Langmuir was found to be a perfect representation of the experimental equilibrium data with high  $R^2$  low RMSE and good  $\chi^2$ . Batch kinetic experiments were carried out and experimental kinetics was fitted by non-linear regression. The sorption process was found to follow the pseudo first-order in case of the three pollutants. This study showed that the activated carbon can be used as a good adsorbent for the removal of phenol derivatives from water according to its maximum adsorption capacity which is about 66.57  $\mu\text{mol/g}$ , 10.42  $\mu\text{mol/g}$  and 5.47  $\mu\text{mol/g}$  respectively for hydroquinone, catechol and resorcinol.

**Keywords:** Activated carbon; adsorption; agricultural residues; phenols; non-linear regression.

## 1. INTRODUCTION

Today, organic matter pollution has become one of the most important environmental problems. It is well known that phenol and its derivatives are the most common organic pollutants in waste waters discharged from petrochemical, chemical and pharmaceutical industries. Among phenol derivatives are hydroquinone, resorcinol and catechol, three isomers of dihydroxybenzene with multiple applications. The wastewater that contains these isomers is harmful to the environment in general and to the aquatic ecosystems in particular. Therefore it must be treated before discharged [1]. The principal techniques used for the removal of phenols are: adsorption using activated carbon [2], wet air catalytic oxidation (WACO) or wet hydrogen peroxide catalytic oxidation (WHPCO) [3], aerobic or anaerobic biodegradation [4].

Activated carbon (AC) is well considered as an excellent adsorbent widely used in purification processes, water treatment, and catalysis [5,6]. Raw materials for activated carbon preparation may be any substance with a relatively high carbon concentration, from mineral carbons to biomass residues [7]. The preparation method involves thermal treatment, with the presence of a chemical agent (chemical method) or activation of carbonizates through controlled gasification (physical method) [8].

Tropical African sub-regions are home to many valuable fruit species whose potentials have not been fully realised. However, tangible economic have been harvested from their wild and/or protected stands in home gardens, farmlands and forest reserves [9]. According to National

Academy of Sciences [10], tropical fruits production in Africa today is being dominated by species introduced from Asia and the Americas, such as bananas, pineapples (*Ananas comosus*), mangos (*Mangifera indica*), papayas (*Carica papaya*), monkey kola and many other. Monkey kola is a common name given to a number of minor relatives of the *Cola* that produce edible tasty fruits. Native people of many countries such as southern Nigeria and Cameroon rely on the fruits of monkey kola, as well as some wild primate animals especially monkeys, baboons and other species. Once emptied of their sweet fruits, monkey cola pods become bulky waste whose open burning pollutes the atmosphere. They should be valued while preserving the environment.

An accurate mathematical description of kinetic study and equilibrium adsorption capacity i.e. the most suitable correlation for the equilibrium curve is vital for reliable prediction of adsorption parameters and quantitative comparison of adsorption behaviour for an adsorbent-adsorbate system in order to optimise the design and to understand the adsorption mechanism [11]. Even though there are considerably many isotherm models available for analysing experimental data and describing the equilibrium of adsorption, there is no general procedure offered to identify a best-fitting adsorption isotherm. Currently, two methods are available such as non-linear regression analysis and linear regression analysis [12,13]. Recently, numerous studies have presented that the linearisation of a non-linear isotherm expression produce different result [14]; In such cases non-linear regression analysis is the only option. Nowadays, this method is used by several researchers to

determine the adsorption isotherm and kinetic parameters [15]. In the case of non-linear regression, the selection of error functions showed a change in the values of individual isotherm and kinetic constants [16]. This could be efficiently pacified by selecting an optimisation procedure such as sum of normalised errors [17]. Therefore, the equilibrium data resulting from batch adsorption experiments is analysed by using different types of isotherm models, the kinetic study by using different types of kinetic models, and a best fit among them is investigated by comparing sum of normalised errors and statistical comparison values. Such a study will be significantly useful in understanding sorption mechanism for the performance of sorption systems.

The aim of this study is to produce activated carbon based on monkey kola pods, an abundant and cost-free resource. The study investigated kinetics and equilibrium aspects of the adsorption of hydroquinone, catechol and resorcinol onto the activated material obtained.

## 2. MATERIALS AND METHODS

### 2.1 Preparation of the Precursor (Raw Adsorbent)

Monkey kola in capsule were purchased in the market of Dschang, a town based in West Cameroon. Initially, the kola was removed from the capsule, the empty capsule washed with distilled water, then cut and dry under the sun until a moisture content less than 10% was obtained; the dried material was then crushed.

### 2.2 Activation of the Precursor

The activated carbon was prepared by chemical activation with orthophosphoric acid ( $H_3PO_4$ ), according to the method developed by Tchakala et al. [18]. The impregnated samples with 18% of  $H_3PO_4$  were carbonised for 2 hrs at  $450^\circ C$ . The activated carbons were labeled MKC.

### 2.3 Characterisation of the Activated Carbon

In order to determine the physicochemical properties of the activated carbon prepared, several analyzes were carried out using for some, usual protocols. These analyses are: Bulk Density, Moisture content [19], Volatile Matter, Iodine Number [20], point of zero charge (pHpzc) [20], pH, Fourier Transform-Infrared (FTIR) Spectroscopy, X-ray diffraction (XRD),

elementary analysis of activated carbon(EDX) and Methylene blue number [21,22].

## 2.4 Reagents

Three Analytical grade reagents (purity > 99 %), were used as adsorbates. A stock solution of each reagent was prepared by dissolving 550 mg of reagent in 50 mL of distilled water. Different initial concentrations were obtained by successive dilutions. Residual concentration of pollutants were determined by UV absorption at 286 nm, 276 nm and 273 nm wavelength respectively for hydroquinone, catechol and resorcinol, using a calibrated UV-Visible spectrophotometer (Jenway model 6715).

## 2.5 Batch Adsorption

Experiments were carried out by dispersing 100 mg of adsorbent in 10 mL of 10-110 mg/L of pollutant solution in 100 mL flasks. The mixture was shaken for 1h, the solution filtered, and the residual concentrations of pollutant determined by spectrophotometry. The amount of pollutant adsorbed was obtained using the following equation:

$$Q_t = \frac{(C_0 - C_t) v}{m} \text{ (mg/g)} \quad (1)$$

Where  $C_0$  and  $C_t$  are the concentrations of pollutant solution (mg/L) at initial and final time (t) respectively; V the volume of solution (mL) and m is the weight (mg) of activated carbon. Each experiment was carried twice and the average results presented.

Experiments were carried out at constant stirring speed of 150 rpm/min. The pH of the medium was adjusted by adding dilute solutions of 0.1 M HCl or 0.1 M NaOH.

## 2.6 Isotherm Studies

During the adsorption process, dynamic equilibrium is established between the pollutants molecules in the aqueous phase and the adsorbent surface at isothermal condition which is expressed by the isotherms. Optimum loading of adsorbents can be easily estimated from these adsorption isotherms [23]. Better insight of the adsorbent-adsorbate binding can be explained by the most fitted isotherms that depend on the nature of the sorption system. Several models were proposed for describing adsorption equilibrium.

### 2.6.1 Langmuir Isotherm

According to the theory of adsorption, the model of Langmuir is based on the fixation of a monolayer of adsorbate molecules on the pores surface [24]. The model assumes uniform adsorption on the surface and no transmigration in the plane of the surface. Langmuir's equation is mathematically expressed as follows.

$$Q_e = \frac{Q_{max}C_eK_L}{1 + C_eK_L} \quad (2)$$

Where:  $K_L$  (L/mg) is the equilibrium adsorption constant and is related to the free energy of the adsorption,  $Q_{max}$  (mg/g), the maximum adsorption capacity  $C_e$ , the equilibrium concentration and  $Q_e$  (mg/g) is the amount adsorbed at equilibrium. A linear form of equation (2) is given in equation (3):

$$\frac{1}{Q_e} = \frac{1}{Q_{max}} + \frac{1}{C_eK_L Q_{max}} \quad (3)$$

### 2.6.1 Freundlich Isotherm

The Freundlich equation is an empirical model that considers heterogeneous adsorptive energies on the adsorbent surface [25].

$$Q_e = K_F C_e^{1/n} \quad (4)$$

The linear form of equation (4) is given in equation (5):

$$\ln Q_e = \frac{1}{n} \ln C_e + \ln K_F \quad (5)$$

Where,  $K_F$  (L/g) and  $1/n$  are Freundlich constants.

### 2.6.2 The Redlich-Peterson Isotherm

The Redlich – Peterson is an empirical isotherm which incorporates three parameters. It may be used to represent adsorption equilibrium over a wide concentration range. It combines some elements from both the Langmuir and Freundlich equation, and consequently, it can be employed either in heterogeneous or homogenous systems. It can be described as follow [26].

$$Q_e = \frac{AC_e}{1 + BC_e^g} \quad (6)$$

Where A (L/g) and B (L/mg) are Redlich–Peterson isotherm constants, g is an exponent which lies between 0 and 1.

### 2.6.3 The Sips Isotherm

The Sips isotherm is a combined form of Langmuir and Freundlich models [27]. At low adsorbate concentrations, this model is reduced effectively to the Freundlich isotherm and did not obey to the Henry's law. At high adsorbate concentrations, it predicts a monolayer sorption capacity which is characteristic of the Langmuir isotherm. The model can be written as:

$$Q_e = \frac{Q_s K_s C_e^{1/n}}{1 + K_s C_e^{1/n}} \quad (7)$$

Where  $Q_s$  (mg/g) is the sips maximum adsorption capacity,  $K_s$  (l/g) is the Sips model isotherm constant, and  $1/n$  is the sips model exponent.

### 2.6.4 The Langmuir-Freundlich Isotherm

The Langmuir-Freundlich isotherm, also known as Sip's equation, is a versatile isotherm expression that can simulate both Langmuir and Freundlich behaviors [28]. The Langmuir-Freundlich isotherm can describe both the Langmuir-type and Freundlich-type adsorption behavior of pollutant and is suitable for modeling pH-dependent sorption effects. A general form of Langmuir-Freundlich isotherm equation can be written as [29]:

$$Q = \frac{Q_m (K_a C_{eq})^n}{1 + (K_a C_{eq})^n} \quad (8)$$

Where, Q is the amount of pollutant adsorbed at equilibrium (mg/g).  $Q_m$  is the adsorption capacity of the system (mg of sorbate/g sorbent).  $C_{eq}$  is the aqueous phase concentration at equilibrium (mg/L).  $K_a$  is the affinity constant for adsorption (L/mg) and n is the index of heterogeneity. Fundamentally, both Langmuir and Freundlich isotherms can be mathematically viewed as the following weighted integral [30]:

$$\int_{-\infty}^{+\infty} g(K_a) \frac{K_a C_{eq}}{1 + K_a C_{eq}} dK_a \quad (9)$$

Where the statistical density function  $g(K_a)$  represents the individual site density values of elementary isotherms with its own affinity constant  $K_a$ . The  $g(K_a)$  distribution reduces to a Dirac's delta function for Langmuir isotherm, and it resembles a log-normal distribution for Freundlich isotherm. The Langmuir-Freundlich isotherm allows one to vary the density function for heterogeneous systems using a

heterogeneity index  $n$ , which is allowed to vary from 0 and 1. The value of  $n$  for a homogeneous material is 1, and it is less than one for heterogeneous materials. Mathematically, when  $n$  is set to 1 the Langmuir-Freundlich isotherm Eq. (8) reduces to the following expression:

$$Q = Q_m \frac{K_a C_{eq}}{1 + K_a C_{eq}} \quad (10)$$

This equation will be identical to the Langmuir isotherm if we replaced  $Q_m$  with  $K_{max}$ , a pH-dependent sorption capacity value. Also, when  $C_{eq}$  or  $K_a$  approaches a low value, the denominator in Eq. (8) will be close to unity and the Langmuir-Freundlich isotherm expression reduces to a Freundlich-type expression [31]. Thus the Langmuir-Freundlich model offers a flexible analytical framework for modeling both Langmuir and Freundlich type sorption effects. Also, the Langmuir-Freundlich isotherm uses a single value to describe the maximum adsorption capacity and does not require fitted adsorption capacity values at different pH values. Instead the value of affinity constant ( $K_a$ ) can be varied to account for pH dependent sorption effects. This approach is consistent with Supplied Chain Management formulations which use a single value for maximum sorption capacity [32].

## 2.7 Kinetics of Adsorption

In order to accurately reflect the variation trend of pollutant concentration with time and reveal the reaction pathway of adsorption process, several kinetic models were employed to examine the experimental data. The nonlinear pseudo-first-order, pseudo-second-order kinetic model, intraparticle and elovich models were expressed as follows:

**Pseudo-first order model:** The pseudo-first-order of Lagergren [33] is expressed as:

$$Q_t = Q_e [1 - \exp(-K_1 t)] \quad (11)$$

Where  $K_1$  ( $mn^{-1}$ ), is the rate constant of pseudo-first order adsorption,  $Q_t$  and  $Q_e$  are respectively the instantaneous and equilibrium amount of pollutant adsorption per unit weight of activated carbon (mg/g) and  $t$  is the time (min). The plot of  $\ln(Q_e - Q_t)$  versus  $t$  should give a linear relationship with the slope equal to  $K_1$ .

**Pseudo-second order model:** The kinetic data are fitted with pseudo-second order model resulting in the following equation [34]:

$$q_t = q_e^2 K_2 t / (1 + q_2 K_2 t) \quad (12)$$

Where  $K_2$  is the rate constant of pseudo-second order.

### Intra-particle diffusion:

Intra-particle diffusion was often considered as the limiting step which limits the kinetics in the process of adsorption. The possibility of a limitation by the diffusion in the pores is explored by plotting pollutant uptake against the square root of time, using the Weber and Morris model:

$$q_t = K_d t^{1/2} + C \quad (13)$$

where  $q_t$  is the instantaneous amount of pollutant adsorption per unit gram of activated carbon (mg/g),  $C$  (mg/g) is a constant giving an idea about the thickness of the boundary layer.

### Elovich kinetic equation:

The Elovich equation is generally expressed as [35]:

$$\frac{dQ_t}{dt} = \alpha e^{-\beta Q_t} \quad (14)$$

where  $Q_t$  (mg/g) is the sorption capacity at time  $t$ ,  $\alpha$  is the initial adsorption rate (mg/g.min), and  $\beta$  is the desorption rate constant (mg/g.min) during any one experiment. The integrated and simplified equation (assuming that  $\alpha\beta t \gg 1$ ) is:

$$Q_t = \frac{1}{\beta} \ln(\alpha\beta) = \frac{1}{\beta} \ln t \quad (15)$$

## 2.8 Non-linear Regression Analysis

Usually, the magnitude of the linear regression coefficient, ( $R^2$ ) is taken as the index for the quality of the fit to the experimental adsorption data. However, transformation of non-linear ones utterly upset their error structure and may also defy the error variance of normality assumptions of standard least squares [36]. Generally, the optimisation procedure required an error function to be able to evaluate the fit of the equation to the experimental data and the isotherm parameters derived can be affected by the choice of the error function [37]. Various error function (HYBRID), derivative of Marquard's percentage standard deviation (MPSD), average relative error (ARE), the sum of absolute errors (RMSE) and non-linear chi-square test ( $\chi^2$ ) can also be used to gauge the goodness of the fit. More detailed definitions of the error function and statistical comparison values are presented in Table 1. These error functions and statistical

comparison values can be evaluated using the tools like solver add-in with Microsoft's spread sheet, Excel through any of the iteration method. The application of these five different error methods will produce different isotherm parameter sets; therefore, it is hard to directly recognise an overall optimum parameter set. In order to facilitate a meaningful comparison between the isotherm parameter sets, the procedure of "sum of the normalised errors"

(SNE) is usually adopted [38]. This approach allows a direct comparison of the scaled errors and thus identifies the isotherm parameter that would provide the closest fit to the measured data. The parameter set derived based on the smallest SNE will be an optimal one provided that there is no bias in the data sampling and type of error functions selected.

**Table 1. Definitions of error functions and statistical comparison values [38]**

Error function	Definition	Remarks
Coefficient of determination (R <sup>2</sup> )	$\left( \frac{(q_{e,meas} - q_{e,Calc})^2}{\sum_{i=1}^p (q_{e,meas} - q_{e,Calc}) + (q_{e,meas} - q_{e,Calc})^2} \right)$	It is used to test the best-fitting isotherms. Its value closer to unity the goodness of the model is perfect
RMSE	$\left( \frac{1}{p-2} \right)^{1/2} \sum_{i=1}^p (q_{e,meas} - q_{e,Calc})^2$	An estimator used to quantify the difference between values implied by calculated and the measured values of the quantify estimated
Non-linear chi square test (χ <sup>2</sup> )	$\sum_{i=1}^p \left( \frac{(q_{e,meas} - q_{e,Calc})^2}{q_{e,meas}} \right) i$	A statistical tool necessary for the best fit of an adsorption system. Small value indicates its similarities while a larger number represents the variation of the experimental data
HYBRID	$\sum_{i=1}^p \left( \frac{(q_{e,meas} - q_{e,Calc})^2}{q_{e,meas}} \right) i$	It was introduced to improve the fit of ERRSQ method at low concentration ranges
MPSD	$\sum_{i=1}^p \left( \frac{(q_{e,meas} - q_{e,Calc})}{q_{e,meas}} \right) z_i$	This function is similar to geometric error distribution which was modified to allow for the number of degrees of freedom of the system
ARE	$\sum_{i=1}^p \left( \frac{q_{e,meas} - q_{e,Calc}}{q_{e,meas}} \right) i$	It shows a under or overestimates the experimental data and attempts to minimise the fractional error distribution across the entire limits of the concentration
EABS	$\sum_{i=1}^p (q_{e,meas} - q_{e,Calc}) i$	A function similar to ERRSQ function, with an increase in the errors will provide a better fit, leading to the bias towards the higher concentration data
ERRSQ	$\sum_{i=1}^p (q_{e,meas} - q_{e,Calc}) i^2$	An error function more helpful at the higher end of the liquid phase concentration ranges. The increasing trend in the magnitude and squares of the errors illustrates a better fit for the deviation of model parameters

The strength of the linear association between two variables is quantified by the square of the correlation coefficient (R) which is called the coefficient of determination (R<sup>2</sup>). Additionally, RMSE and Non-linear chi-square test were used to determine the linear relationship strength and to measure the accuracy of predictions. These three error functions were also applied to discuss the fitness of isotherm and kinetic models, and to select the best model which fits to experimental data.

### 3. RESULTS AND DISCUSSION

#### 3.1 Characterization of Activated Carbon

Table 2 gives the properties of the activated carbon produced in this study.

The bulk density of the activated carbon is 467.8kg/m<sup>3</sup>. The activated carbon presents an acid pH value and an acid point of zero charge.

#### 3.2 Iodine Number

High values of iodine number indicate high degree of activation in the surface area. It is a measure of the micropores and it is used as an indication of the total surface area [19, 39]. The iodine numbers of activated carbon prepared in this investigation is 587.2 mg/g. This value indicates that the activated carbon performs well in removing small sized contaminants. Table 3 compares iodine numbers of the present work with other known iodine numbers.

#### 3.3 Infra-red Analysis

Fig. 1 gives the FTIR-spectra of monkey kola waste before carbonisation and Fig. 2 represents the FTIR-spectra of the activated carbon MKC.

In the raw material samples, the O-H stretching vibration bands seen in the wavenumber range of 3800-3000 cm<sup>-1</sup> indicate the presence of surface hydroxyl groups of alcohol, water and polysaccharides. The presence of absorption bands characteristic of CH, or CH<sub>2</sub> structures (2100- 2300 cm<sup>-1</sup>and 1400-1000 cm<sup>-1</sup>) in all the spectra suggests the existence of some aliphatic species. The presence of bands in the range 1600-1400 cm<sup>-1</sup> can be attributed to the stretching vibrations of C=O in carboxylics, esters, lactones, quinones and/or ion radical structures. Also, the 1700 cm<sup>-1</sup> adsorption bands was attributed to C=C of alkene and carboxylate structures. The absorption bands in the 1710-1600 cm<sup>-1</sup>, 1550-1510 cm<sup>-1</sup>and 1500-1520 cm<sup>-1</sup> regions are due to aromatic rings and double bond vibrations. The C-O single bond shows an adsorption band [45] at about 1000 cm<sup>-1</sup>.

In the FTIR spectrum of activated carbon the presence of absorption bands characteristic of CH or CH<sub>2</sub> structures (2700-2800 cm<sup>-1</sup> and 500-530 cm<sup>-1</sup>) suggests the existence of some aliphatic species in the activated carbon [46]. The presence of bands at 1400 cm<sup>-1</sup> can be attributed to the stretching

**Table 2. Characterisation of the adsorbent**

Sample	Bulk density, (kg/m <sup>3</sup> )	Moisture content (%)	pH	PHpcz	Iodine number (mg/g)	Methylene blue adsorption (mg/g)
MKC	467.8	7	6.01	6.87	587.2	147.76

**Table 3. Iodine number of some activated carbon**

Samples	Iodine number	References
MKC	587.2	Present work
Comercial activated carbon	585.00	[40]
Coconut shell activated carbon 750S100	478	[41]
Coconut shell activated carbon 750S100	562	[41]
Coconut shell activated carbon 800S30	682	[41]
Corn Cobs activated carbon	447.7	[42]
Coffee husk activated carbon	457.2	[42]
Cassava peel activated carbon	306.4	[43]
Cola acuminate carbon	656.71	[44]

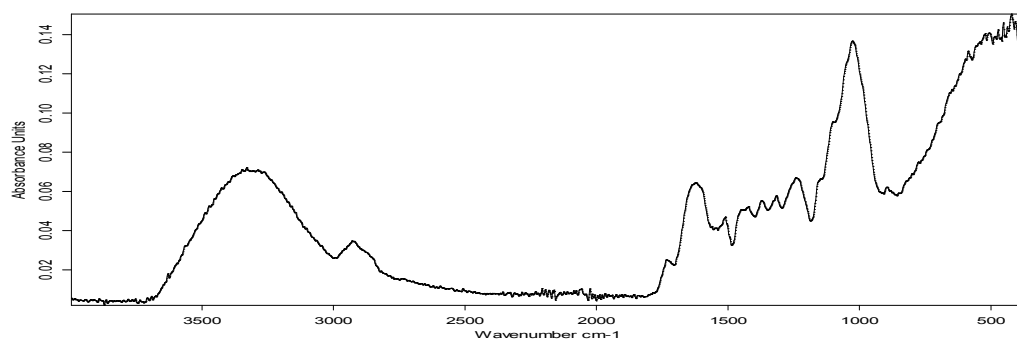


**Fig. 1. FTIR spectra of monkey kola waste**

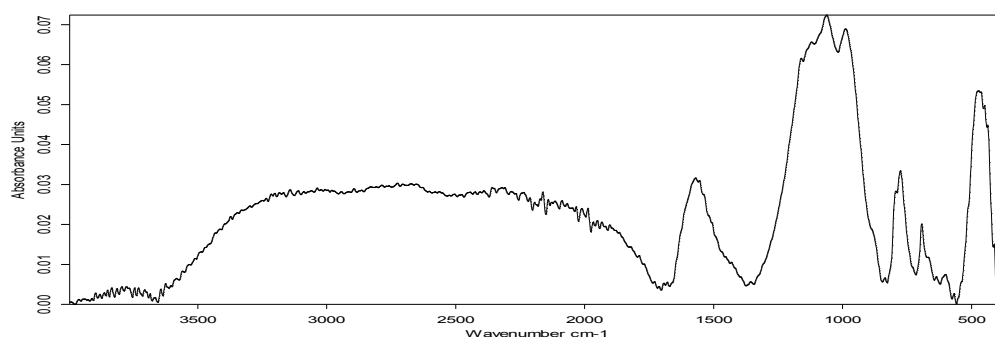


**Fig. 2. FTIR spectra of activated carbon MKC**

vibrations of C=O in carboxylic acids. Another broad band in the 1200-1400  $\text{cm}^{-1}$  range consisting of a series of overlapping absorption bands that can be ascribed to C=C of aromatics ring [47]. The overlapping peaks which form an absorption band in the 1700-1400  $\text{cm}^{-1}$  region, can be assigned to C-O of carboxylic acid, phenolic structures and esters. After the activation with  $\text{H}_3\text{PO}_4$ , the peak at the 3500-3100  $\text{cm}^{-1}$  range of the precursor becomes weaker indicating the disappearance of water molecules. Several new peaks are detected in the region of 700–850  $\text{cm}^{-1}$ . There might also contain phosphorus.

### 3.4 X-ray Diffraction Analysis

Fig. 3 gives the XRD-spectra of monkey kola waste before carbonisation and the XRD-spectra of the activated carbon MKC. This pattern generally shows an amorphous structure of materials and a low crystallinity of sample in the range of 5 to 48°. For the raw materials, the diffraction patterns show a peak at 22° which is attributed to the presence of the native cellulose.

The diffraction patterns of activated MKC show almost the same pattern and exhibit the same diffraction peaks at 25 and 43° which are attributed respectively to the presence of carbon / graphite and dehydrated hemicellulose [48]. On the other hand we find that after activation of the raw materials, the main peak moves from 22 to 25° and the appearance of a peak at 39°, which shows that the activation process was well done.

### 3.5 Elemental Analysis

Elemental analysis help to determine the proportions of nitrogen, carbon, hydrogen and sulfur atoms present in each material. The Table 4 shows the result of elemental analysis of monkey kola waste and the activated carbon MKC.

It appears that the carbonised material is richer in carbon atoms than the raw material. The carbon content has almost doubled in activated carbon MKC, which is consistent with expectations.



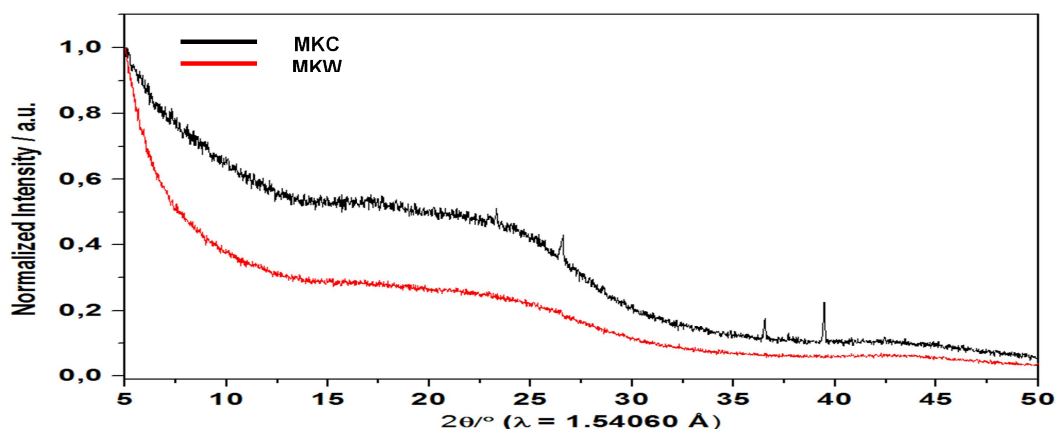


Fig. 3. X-ray diffraction patterns of monkey kola waste and activated carbon MKC

Table 4. Elemental analysis of monkey kola waste and activated carbon MKC

Sample	N %	C %	H %	S %	Weight
Blank	0	0	0	0	1
monkey kola waste	2.2	40.2	3.4	0	2.1
MKC	2.6	66.6	2.9	0	2.5

### 3.6 Adsorption Studies

#### 3.6.1 Effect of contact time

The effect of contact time on the removal of the three pollutants is reported in Fig. 4. The result indicates that the equilibrium time was reached after about 30 minutes. It was observe that adsorption reaction was rapid in the first 15 min, followed by a sluggish stage until equilibrium. The adsorption of the three pollutants involve three steps: a rapid external surface diffusion process (step 1): This is due to the fact that

initially the number of sites of activated carbon available is higher and the driving force for the mass transfer is greater. A slow intraparticle diffusion stage (step 2): In the second region (15-30 minutes), as the time progresses, the number of free sites on the activated carbon decreases, and the non-adsorbed molecules are assembled at the surface, thus limiting the adsorption capacity and the rate. And a dynamic adsorption-desorption equilibrium (step 3): at this step, the equilibrium is already reach. These three processes often occurred simultaneously.

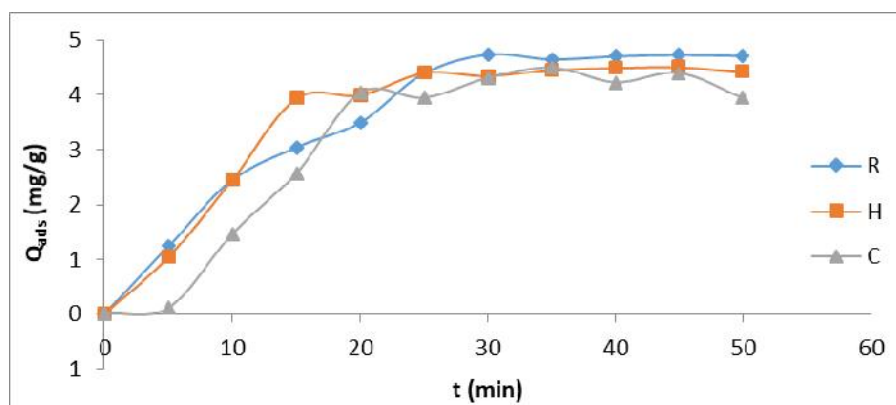


Fig. 4. Effect of contact time on the uptake of hydroquinone, catechol and resorcinol onto the activated carbon MKC (room temperature, 55.55 mg/L initial concentration, pH = 7)

### 3.6.2 Effect of initial pH on the adsorption

The pH of solution is one of the most important parameters that affect the adsorption process, because it affects the surface charge of the adsorbent as well as the degree of ionisation and speciation of our pollutants [49]. The effect of initial pH on the adsorption of hydroquinone, catechol and resorcinol was studied with initial pollutant concentration of 55.55 mg/L and optimum carbon amount of 0.1 g. Fig. 5 shows the influence of solution pH on the three pollutants removed by MKC at a pH range 2.0 to 14.0. The result shows that the quantity of pollutant adsorbed increased from 2 to 6; and then decreased sharply (pH>8). The maximum pollutant uptake obtained between pH = 6 and 8 can be explained by the fact that at these pH, more protonated species are present in the solution. At pH = 10, the repulsive electrostatic forces predominate, and the adsorption at low

concentrations is less than that at high concentrations.

### 3.6.3 Effect of amount of adsorbent

Another parameter that controls adsorption is the amount of activated carbon employed. Under selected conditions (stirring time of 30 minutes and pollutant concentration of 55.55 mg/L), the amount of activated carbon was varied from 10 mg to 100 mg. Fig. 6 indicates that the adsorption amount increases as the amount of activated carbon increases. This is due to the fact that, an increase in the mass increases the number of sites of adsorption on the surface of the adsorbent. At 100 mg of activated carbon, almost 97.94% of the pollutant was removed from solutions in the case of hydroquinone, 98.8% in the case of catechol and 97.04 in the case of resorcinol. Hence, for subsequent studies, 100 mg of activated carbon was used.

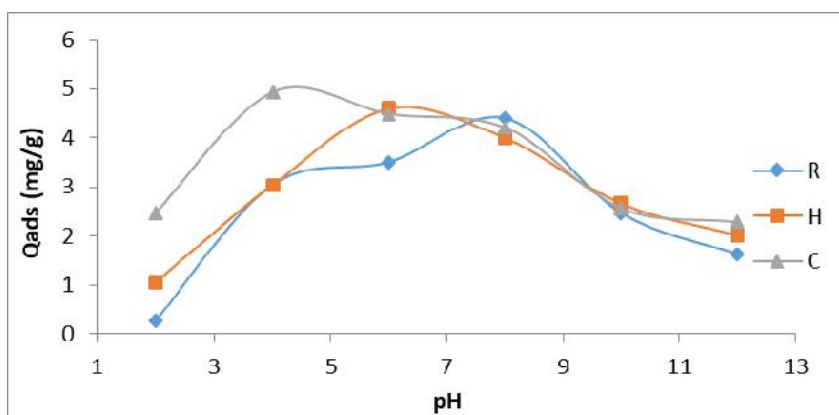


Fig. 5. Effect of pH on the uptake of hydroquinone, catechol and resorcinol onto the activated carbon MKC (room temperature, 55.55 mg/L initial concentration)

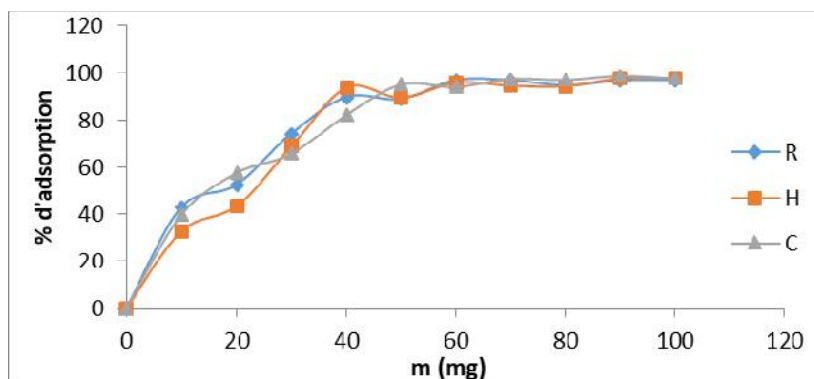


Fig. 6. Effect of amount of adsorbent on the uptake of hydroquinone, catechol and resorcinol onto the activated carbon MKC (room temperature, 55.55 mg/L initial concentration).

### 3.6.4 Kinetic study

Kinetic methods are generally used to determine the rate and elucidate the mechanism of the reactions [32]. To evaluate the kinetic mechanism that controls the adsorption process of hydroquinone, catechol and resorcinol on the activated carbon, the pseudo-first order, the pseudo-second order, Elovich and intra-particle diffusion model were tested to interpret the experimental data. Non-linear kinetic models are being fitted (Figs. 7, 8, 9) and kinetic data estimated (Table 5).

Non-linear pseudo first order model was applied to accurately reflect the variation trend of pollutant concentration with time and reveal the reaction pathway of adsorption process. The pseudo-first order model well described the adsorption data for all the three adsorbents as evidenced by high coefficients of determination  $R^2$  (0.962), low RMSE (0.915) and good  $\chi^2$  (0.355) values, in the case of hydroquinone; with high  $R^2$  (0.923), low RMSE (1,287) and good  $\chi^2$  (0.504) values, in the case of catechol; and with high  $R^2$  (0.986), low RMSE (0,608) and good  $\chi^2$  (0.101) values, in the case of resorcinol (Table 5). Thus, it can be concluded that adsorption speed of the three pollutants onto MKC is proportional to the number of adsorption sites, involving forces caused by the sharing of electrons between activated carbon and pollutants [50]. In addition, the predicted equilibrium adsorption capacities ( $Q_e$ ) for hydroquinone, catechol and resorcinol were 4.702 mg/g, 4.708 mg/g and 5.127 mg/g respectively. These results show that the sorption of hydroquinone, catechol and resorcinol from aqueous solution onto activated carbon MKC follows the pseudo-first kinetic model and

could be used to determine the equilibrium sorption capacity, rate constant and percentage of these pollutants removal. Intraparticle diffusion model was applied to describe experimental data obtained for the adsorption of the three pollutants onto carbon MKC (Figs. 7, 8 and 9). The relatively low values of  $R^2$  (0.849; 0.863 and 0.931) RMSE (1.813; 1.858 and 1.351) and  $\chi^2$  (1.342; 0.641 and 0.656) respectively for hydroquinone, catechol and resorcinol indicated that this model utterly failed to predict the equilibrium data (Table 5). According to the  $R^2$ , RMSE and  $\chi^2$  values, the best-fitted adsorption kinetic models were found in the order: pseudo first order > pseudo second order > Elovich > intraparticle diffusion.

### 3.6.5 Equilibrium isotherm modeling

The adsorption isotherm was obtained from data deduced from the effect of initial pollutant concentration. These isotherms are generally used to establish the relationship between the amount of pollutant adsorbed and its equilibrium concentration in solution. Although these isotherms do not lead to the deduction of the adsorption mechanisms they are useful for comparing results from different sources on a quantitative basis, providing information on the adsorption potential of a material with easily interpretable constants.

After choosing the overall best error method for determining the parameters of the isotherm models, the plots of different non-linear isotherm models with optimised values of the constants were presented in Figs. 10, 11 and 12, and calculated isotherm data are presented in Table 6.

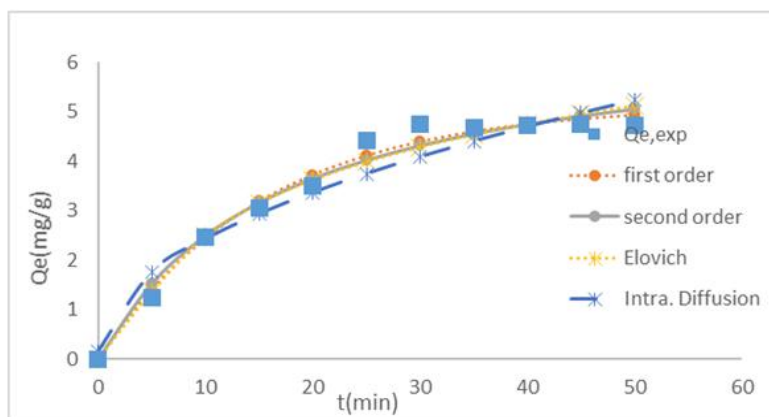


Fig. 7. non-linear kinetic study of resorcinol removal onto the activated carbon MKC

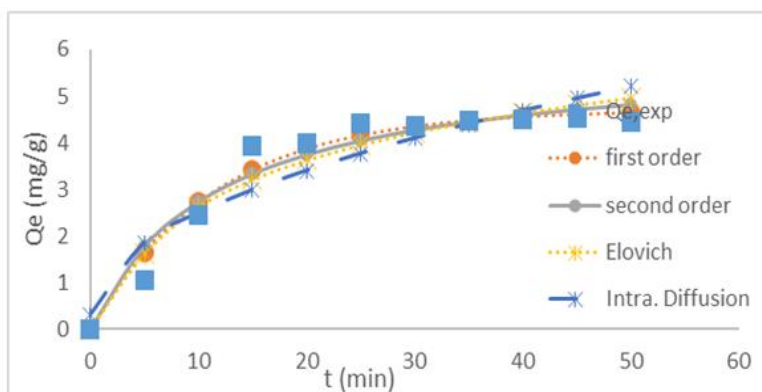


Fig. 8. Non-linear kinetic study of hydroquinone removal onto the activated carbon-MKC

Table 5. Kinetic parameters of different models

N°	Models	Constants	Values	R <sup>2</sup>	RMSE	χ <sup>2</sup>
<b>Resocinol</b>						
1.	Pseudo first order	Q <sub>e</sub> (mg/g)	5.127	0.986	0.608	0.101
		K <sub>1</sub> (1/min)	0.0660			
2.	Pseudo second order	Q <sub>e</sub> (mg/g)	6.789	0.976	0.775	0.171
		K <sub>2</sub> (g/min.mg)	0.0085			
3.	Elovich	α (mg/g.min)	0.7495	0.954	0.804	0.154
		β (g/mg)	0.6123			
4.	Intraparticle diffusion	K <sub>p</sub> (mg/g.min <sup>0.5</sup> )	0.718	0.931	1.351	0.656
		C (mg/g)	0.151			
<b>Hydroquinone</b>						
1.	Pseudo first order	Q <sub>e</sub> (mg/g)	4.702	0.962	0.915	0.355
		K <sub>1</sub> (1/min)	0.0863			
2.	Pseudo second order	Q <sub>e</sub> (mg/g)	5.941	0.938	1.167	0.524
		K <sub>2</sub> (g/min.mg)	0.0142			
3.	Elovich	α (mg/g.min)	0.8757	0.8597	1.271	0.540
		β (g/mg)	0.6842			
4.	Intraparticle diffusion	K <sub>p</sub> (mg/g.min <sup>0.5</sup> )	0.692	0.849	1.813	1.342
		C (mg/g)	0.300			
<b>Cathecol</b>						
1.	Pseudo first order	Q <sub>e</sub> (mg/g)	4.708	0.923	1.287	0.554
		K <sub>1</sub> (1/min)	0.0624			
2.	Pseudo second order	Q <sub>e</sub> (mg/g)	7.012	0.901	1.493	0.674
		K <sub>2</sub> (g/min.mg)	0.0058			
3.	Elovich	α (mg/g.min)	0.6166	0.8352	1.469	0.663
		β (g/mg)	0.6313			
4.	Intraparticle diffusion	K <sub>p</sub> (mg/g.min <sup>0.5</sup> )	0.744	0.863	1.858	0.641

As can be seen from all the figures, the curve of Langmuir was the most consistent with a high R<sup>2</sup> (0.988; 0.934 and 0.978), a good χ<sup>2</sup> (0.542; 0.589 and 0.089) and a low RMSE (3.491; 1.245 and 0.447) respectively in the case of hydroquinone, catechol and resorcinol, followed by Langmuir-Freundlich isotherm, with a high R<sup>2</sup> (0.988; 0.964 and 0.978), a good χ<sup>2</sup> (0.522; 0.777 and 0.1) and a low RMSE (3.485; 1.000

and 0.434) respectively in the case of hydroquinone, catechol and resorcinol.

The Langmuir isotherm is the most appropriate model describing the three pollutants adsorption. This suggests that the adsorption covers a monolayer of the carbon surface and there is not interaction between adsorbed molecules.

Comparing the maximum adsorption capacity,  $Q_m$ , of the 3 isomers, (Table 6) it is found that hydroquinone is more adsorbed: 66.5  $\mu\text{mol/g}$  against 10.4 for catechol and 5.5 for resorcinol. Previous studies confirm the low adsorption of resorcinol compared with catechol [51,52]. The explanation lies in the solubility and spatial configuration of these isomers. Indeed, resorcinol is more soluble than catechol and catechol more

soluble than hydroquinone. The more soluble a substance is, the less it is adsorbed. The position of hydroxides on benzene also influences adsorption. Indeed, hydroquinone is a symmetrical molecule according to the position 1-4 of hydroxides on benzene. This configuration allows it to access the adsorption sites more easily and energetically favorable because of its greater stability.

**Table 6. Parameters of isotherm adsorption of hydroquinone, catechol and resorcinol**

N°	Models	Constants	Values	R <sup>2</sup>	RMSE	$\chi^2$
<b>Hydroquinone</b>						
1.	Langmuir	$Q_m$ ( $\mu\text{mol/g}$ )	66.567	0.988	3.491	0.542
		$K_L$	0.282			
2.	Freundlich	$K_F$	14.888	0.979	4.558	1.348
		$N$	1.612			
3.	Redlich-Peterson	$A$ (L/g)	19.281	0.988	3.488	0.555
		$B$ (L/ $\mu\text{mol}$ )	0.313			
		$B$	0.961			
4.	Sips	$q_{m_s}$ ( $\mu\text{mol/g}$ )	64.056	0.988	3.485	0.522
		$K_s$ (L/ $\mu\text{mol}$ )	0.295			
		$\beta_s$	1.027			
5.	Langmuir-Freundlich	$Q_m$ ( $\mu\text{mol/g}$ )	64.055	0.988	3.485	0.522
		$K_{LF}$	0.305			
		$M_{LF}$	1.027			
<b>Cathecol</b>						
1.	Langmuir	$Q_m$ ( $\mu\text{mol/g}$ )	10.416	0.934	1.245	0.589
		$K_L$	0.212			
2.	Freundlich	$K_F$	1.816	0.907	1.464	0.860
		$N$	1.459			
3.	Redlich-Peterson	$A$ (L/g)	4.519	0.917	1.408	0.770
		$B$ (L/ $\mu\text{mol}$ )	1.411			
		$B$	0.472			
4.	Sips	$Q_{m_s}$ ( $\mu\text{mol/g}$ )	70.214	0.892	1.479	0.946
		$K_s$ (L/ $\mu\text{mol}$ )	0.029			
		$\beta_s$	0.665			
5.	Langmuir-Freundlich	$Q_m$ ( $\mu\text{mol/g}$ )	5.826	0.964	1.007	0.777
		$K_{LF}$	0.575			
		$M_{LF}$	1.984			
<b>Resorcinol</b>						
1.	Langmuir	$Q_m$ ( $\mu\text{mol/g}$ )	5.471	0.978	0.447	0.089
		$K_L$	0.554			
2.	Freundlich	$K_F$	1.930	0.965	0.541	0.195
		$N$	2.021			
3.	Redlich-Peterson	$A$ (L/g)	3.956	0.979	0.419	0.096
		$B$ (L/ $\mu\text{mol}$ )	1.016			
		$B$	0.822			
4.	Sips	$Q_{m_s}$ ( $\mu\text{mol/g}$ )	6.338	0.978	0.434	0.100
		$K_s$ (L/ $\mu\text{mol}$ )	0.444			
		$\beta_s$	0.869			
5.	Langmuir-Freundlich	$q_{mif}$ ( $\mu\text{mol/g}$ )	6.339	0.978	0.434	0.100

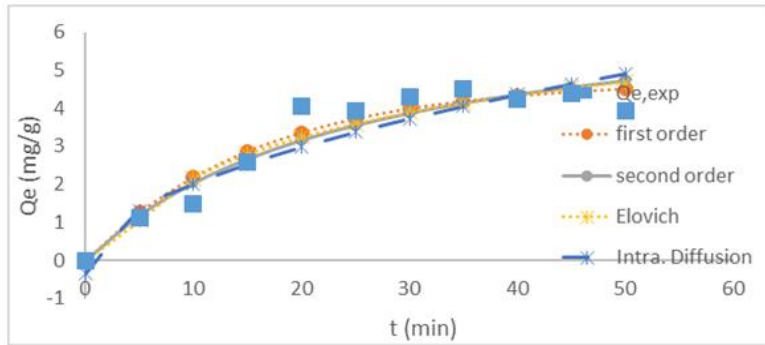


Fig. 9. Non-linear kinetic study of catechol removal onto the activated carbon MKC

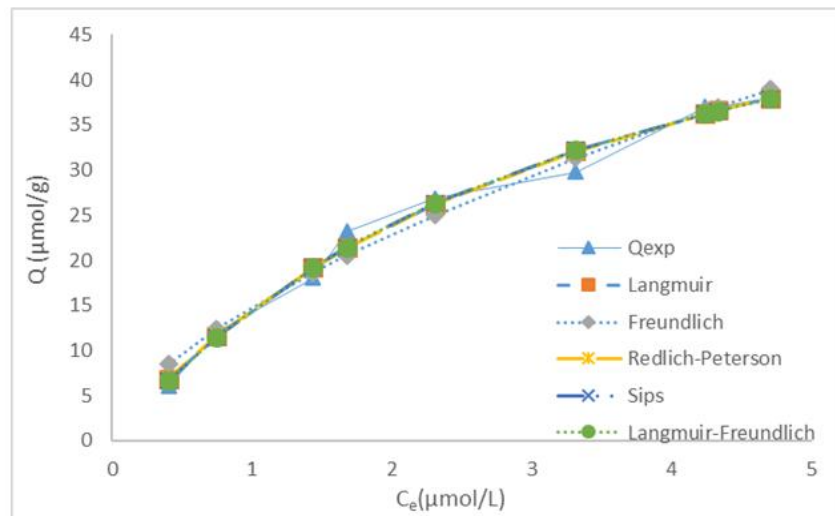


Fig. 10. Non-linear adsorption isotherm of hydroquinone removal onto the activated carbon MKC

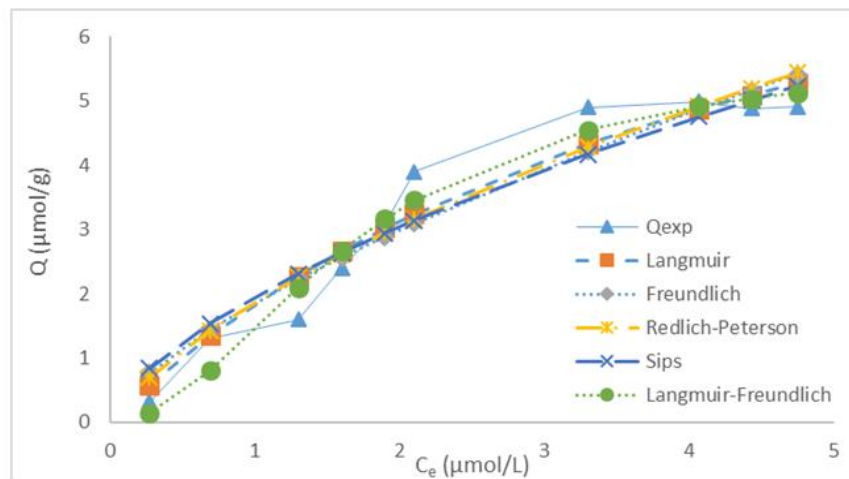
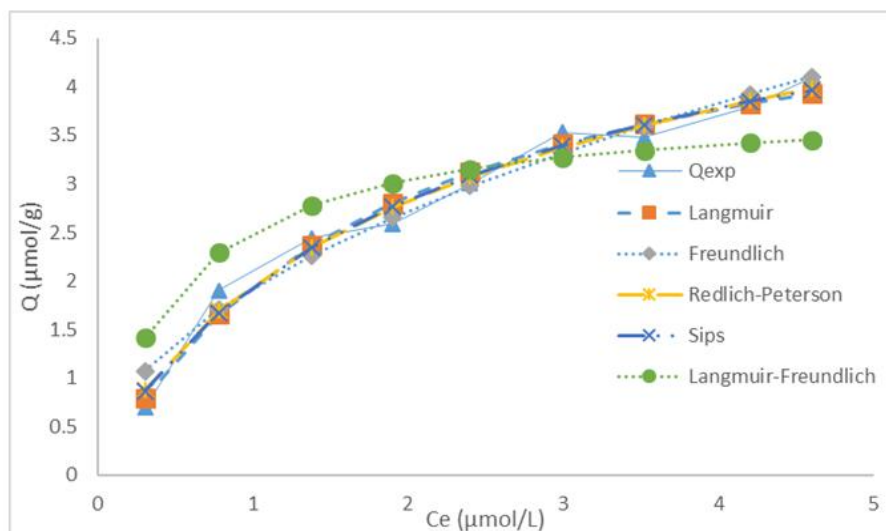


Fig. 11. Non-linear adsorption isotherm of catechol removal onto the activated carbon MKC



**Fig. 12. Non-linear adsorption isotherm of Resorcinol removal onto the activated carbon MKC**

#### 4. CONCLUSION

Activated carbon was prepared from waste of monkey kola by pyrolysis and chemical activation with phosphoric acid  $H_3PO_4$  at  $450^\circ C$  for 2 hours. The prepared activated carbon was characterised by determining different parameters such as Iodine number, methylene blue number, FT-IR and EDX spectroscopy. This carbon was evaluated as adsorbent for the removal of hydroquinone, catechol and resorcinol in solution. The adsorption experiments were performed as a function of adsorbent dosage, pH and contact time. The percentage of removal increased with increasing contact time and dose of the adsorbent. Furthermore, the kinetics of the adsorption studies were fitted to a pseudo-first-order kinetic model at different concentrations. The equilibrium data were well-expressed by the Langmuir isotherm model. The present study suggests that activated carbon from waste of monkey kola is a low-cost and environmental friendly adsorbent that may be used for the removal of phenolic compounds from aqueous solutions.

#### COMPETING INTERESTS

Authors have declared that no competing interests exist.

#### REFERENCES

1. Rengaraj S, Moon SH, Sivabalan R, Arabindoo B, Murugesan V. Agricultural solid waste for the removal of organics: Adsorption of phenol from water and wastewater by palm seed coat activated carbon. *Waste Manag.* 2002;22:543–548. Available: [https://doi.org/10.1016/S0956-053X\(01\)00016-2](https://doi.org/10.1016/S0956-053X(01)00016-2)
2. Molina-Sabio M. Phosphoric acid activated carbon discs for methane adsorption. *Carbon N.Y.* 2003;41:2113–2119. Available: [https://doi.org/10.1016/S0008-6223\(03\)00237-9](https://doi.org/10.1016/S0008-6223(03)00237-9)
3. Eftaxias A, Font J, Fortuny A, Fabregat A, Stüber F. Catalytic wet air oxidation of phenol over active carbon catalyst. Global kinetic modelling using simulated annealing. *Appl. Catal. B Environ.* 2006;67: 12–23. Available: <https://doi.org/10.1016/j.apcatb.2006.04.012>
4. Agarry SE, Durojaiye AO, Yusuf RO, Aremu MO, Solomon BO, Mojeed O. Biodegradation of phenol in refinery wastewater by pure cultures of *Pseudomonas aeruginosa* NCIB 950 and *Pseudomonas fluorescens* NCIB 3756. *Int. J. Environ. Pollut.* 2008;32:3. Available: <https://doi.org/10.1504/IJEP.2008.016894>
5. Ekpote OA, Horsfall M. Kinetic sorption study of phenol onto activated carbon derived from fluted pumpkin stem waste (*Telfairia occidentalis* Hook. F). *ARPN J. Eng. Appl. Sci.* 2011;6:43–49.
6. Schüth EF, Sing K, Weitkamp J. Surface composition and structure of active

- carbons. *Handb. Porous Solids*. 2002;1–17.  
Available:<https://doi.org/10.1002/9783527618286>
7. Menendez-Diaz JA, Martin-Güllon J. Types of carbons adsorbents and their production. *Activated carbon Surfaces in Environmental Remediation*, T.J. Badosz (editor), Elsevier Ltd; 2006;1- 42.
  8. Bansal RC, Goyal M. *Activated carbon adsorption*. Taylor & Francis Group, LLL. 2005;472.
  9. Okigbo BN. Neglected plants of horticultural and nutritional importance in traditional farming systems of tropical Africa. *IV Africa Symp. Hortic. Crop*. 1977;53.  
Available:[https://doi.org/http://www.actahort.org/books/53/53\\_18.htm](https://doi.org/http://www.actahort.org/books/53/53_18.htm)
  10. National Academy of Sciences. *Lost Crops of Africa: Fruits*. Washington D.C. USA: National Academies Press. 2008;3:381.  
Available:[www.nap.edu.catalog.php?record\\_id=11879](http://www.nap.edu/catalog.php?record_id=11879)
  11. Ho YS, Porter JF, McKay G. Divalent metal ions onto peat: Copper, nickel and lead single component systems. *Water, Air, Soil Pollut*. 2002;141:1–33.  
Available:<https://doi.org/10.1023/A:1021304828010>
  12. Foo BHK. Insights into the modeling of adsorption isotherm systems. *Chem. Eng. J*. 2010;156:2–10.  
Available:<https://doi.org/doi:10.1016/j.cej.2009.09.013>
  13. Porter JF, McKay G, Choy KH. The prediction of sorption from a binary mixture of acidic dyes using single- and mixed-isotherm variants of the ideal adsorbed solute theory. *Chem. Eng. Sci*. 1999;54: 5863–5885.  
Available:[https://doi.org/10.1016/S0009-2509\(99\)00178-5](https://doi.org/10.1016/S0009-2509(99)00178-5)
  14. Shikuku VO, Kowenje CO, Kengara. Errors in parameters estimation using linearized adsorption isotherms: Sulfadimethoxine adsorption onto kaolinite clay. *Chem. Sci. Inter. J*. 2018;23(4):1-6.
  15. Bilgili MS. Adsorption of 4-chlorophenol from aqueous solutions by xad-4 resin: Isotherm, kinetic, and thermodynamic analysis. *J. Hazard. Mater*. 2006;137:157–164.  
Available:<https://doi.org/10.1016/J.JHAZMAT.2006.01.005>
  16. Othman MR, Amin AM. Comparative analysis on equilibrium sorption of metal ions by biosorbent Tempe. *Biochem. Eng. J*. 2003;16:361–364.  
Available:[https://doi.org/10.1016/S1369-703X\(03\)00111-6](https://doi.org/10.1016/S1369-703X(03)00111-6)
  17. Wong YC, Szeto YS, Cheung WH, McKay G. Adsorption of acid dyes on chitosan - Equilibrium isotherm analyses. *Process Biochem*. 2004;39:693–702.  
Available:[https://doi.org/10.1016/S0032-9592\(03\)00152-3](https://doi.org/10.1016/S0032-9592(03)00152-3)
  18. Tchakala I, Bawa L, Djaneye-Boundjou G, Doni K, Nambo P. Optimisation du procédé de préparation des Charbons Actifs par voie chimique ( $H_3PO_4$ ) à partir des tourteaux de Karité et des tourteaux de Coton. *Int. J. Biol. Chem. Sci*. 2012;6: 461–478.  
Available:<https://doi.org/10.4314/ijbcs.v6i1.42>
  19. ASTM. Standard Test Method for Moisture in Activated Carbon. *Chem. Sci. Trans*. 1999;6:461–478.
  20. Lopez-Ramon MV, Stoeckli F, Moreno-Castilla C, Carrasco-Marin F. On the characterization of acidic and basic surface sites on carbons by various techniques. *Carbon N. Y*. 1999;37:1215–1221.  
Available:[https://doi.org/10.1016/S0008-6223\(98\)00317-0](https://doi.org/10.1016/S0008-6223(98)00317-0)
  21. Nunes CA, Guerreiro MC. Estimation of surface area and pore volume of activated carbons by methylene blue and iodine numbers. *Quim. Nova*. 2011;34:472–476.  
Available:<https://doi.org/10.1590/S0100-40422011000300020>
  22. Zhang J, Xie S, Ho YS. Removal of fluoride ions from aqueous solution using modified attapulgite as adsorbent. *J. Hazard. Mater*. 2009 ;165:218–222.  
Available:<https://doi.org/10.1016/j.jhazmat.2008.09.098>
  23. Akar T, Tunali S. Biosorption characteristics of *Aspergillus flavus* biomass for removal of Pb(II) and Cu(II) ions from an aqueous solution. *Bioresour. Technol*. 2006;97:1780–1787.  
Available:<https://doi.org/10.1016/j.biortech.2005.09.009>
  24. Langmuir I. The adsorption of gases on plane surfaces of glass, mica and platinum. *J. Am. Chem. Soc*. 1918;40: 1361–1403.  
Available:<https://doi.org/10.1021/ja02242a004>



25. Yang RT. Adsorbents Fundamentals and Applications; 2003.
26. Repo E, Malinen L, Koivula R, Harjula R, Sillanpää M. Capture of Co(II) from its aqueous EDTA-chelate by DTPA-modified silica gel and chitosan. *J. Hazard. Mater.* 2011;187:122–132.  
Available:<https://doi.org/10.1016/j.jhazmat.2010.12.113>
27. Sips R. On the structure of a catalyst surface. *J. Chem. Phys.* 1948;16:490–495.  
Available:<https://doi.org/10.1063/1.1746922>
28. Nahm MH, Herzenberg LA, Little K. A New method of applying the Sips equation. *J. Immunol.* 1977;119:301–305.
29. Turiel E, Perez-Conde C, Martin-Esteban A. Assessment of the cross-reactivity and binding sites characterisation of a propazine-imprinted polymer using the Langmuir-Freundlich isotherm. *Analyst.* 2003 ;128:137–141.  
Available:<https://doi.org/10.1039/b210712k>
30. Limousin G, Gaudet JP, Charlet L, Szenknect S, Barthès V, Krimissa M. Sorption isotherms: A review on physical bases, modeling and measurement. *Appl. Geochemistry.* 2007;22:249–275.  
Available:<https://doi.org/10.1016/j.apgeochem.2006.09.010>
31. Umpleby RJ, Baxter SC, Chen Y, Shah RN, Shimizu KD. Characterization of molecularly imprinted polymers with the Langmuir - Freundlich isotherm. *Anal. Chem.* 2001;73:4584–4591.  
Available:<https://doi.org/10.1021/ac0105686>
32. Jeppu GP, Clement TP. A modified Langmuir-Freundlich isotherm model for simulating pH-dependent adsorption effects. *J. Contam. Hydrol.* 2012 ;129–130: 46–53.  
Available:<https://doi.org/10.1016/j.jconhyd.2011.12.001>
33. Srivastava VC, Swamy MM, Mall ID, Prasad B, Mishra IM. Adsorptive removal of phenol by bagasse fly ash and activated carbon: Equilibrium, kinetics and thermodynamics. *Colloids Surfaces A Physicochem. Eng. Asp.* 2006;272:89–104.  
Available:<https://doi.org/10.1016/j.colsurfa.2005.07.016>
34. Srihari V, Das A. The kinetic and thermodynamic studies of phenol-sorption onto three agro-based carbons. *Desalination.* 2008;225:220–234.  
Available:<https://doi.org/10.1016/j.desal.2007.07.008>
35. Gaid A, Kaoua F, Mederres N, Khodja M. Surface mass transfer processes using activated date pits as adsorbent. 1994;20: 4738.
36. El-Khaiary MI. Least-squares regression of adsorption equilibrium data: Comparing the options. *J. Hazard. Mater.* 2008;158:73–87.  
Available:<https://doi.org/10.1016/j.jhazmat.2008.01.052>
37. Brown AM. A step-by-step guide to non-linear regression analysis of experimental data using a Microsoft Excel spreadsheet. *Comput. Methods Programs Biomed.* 2001;65:191–200.  
Available:[https://doi.org/10.1016/S0169-2607\(00\)00124-3](https://doi.org/10.1016/S0169-2607(00)00124-3)
38. Kundu S, Gupta AK. Arsenic adsorption onto iron oxide-coated cement (IOCC): Regression analysis of equilibrium data with several isotherm models and their optimization. *Chem. Eng. J.* 2006;122:93–106.  
Available:<https://doi.org/10.1016/j.cej.2006.06.002>
39. Devi VB, Jahagirdar AA, Zulficar AMN. Adsorption of Chromium on activated carbon prepared from coconut shell. *International Journal of Engineering Research and Applications.* 2012;2:364-370.
40. Ilaboya IR, Oti EO, Ekoh GO, LOU. The role of renewable energies in sustainable development: Case study Iran. *Iran. J. Energy Environ.* 2013;4:320–329.  
Available:<https://doi.org/10.5829/idosi.ijee.2013.04.04>.
41. Devi B, Jahagirdar A, Ahmed M. Adsorption of chromium on activated carbon prepared from coconut shell. *Adsorption.* 2012 ;2:364–370.
42. Nono PN, Kamgaing T, Raoul D. Optimisation of catechol removal from aqueous solution by adsorption on activated carbon from corn cobs and coffee husk. *Chem. Sci. Trans.* 2016;5.  
Available:<https://doi.org/10.7598/cst2016.1247>
43. Nwabanne JT, Igbokwe PK. Kinetics and Equilibrium Modeling of nickel adsorption by cassava peel. *J. Eng. Appl. Sci;* 2008.
44. Ndi JN, Ketcha JM, Anagho SG, Goghomo JN, Bilibi BPD. Physical and chemical characteristics of activated carbon

- prepared by pyrolysis of chemically treated Cola nut (*Cola acuminata*) Shells wastes and its ability to adsorb organics. Int. J. Adv. Chem. Technol. 2014;3:1–13.
45. Meldrum BJ, Rochester CH. *In situ* infrared study of the surface oxidation of activated carbon in oxygen and carbon dioxide. J. Chem. Soc. Faraday Trans. 1990;86:861–865.  
Available: <https://doi.org/10.1039/FT9908601881>
46. Dong Jin Suh, Tae-Jin P, Son-Ki I. Effect of surface oxygen groups of carbon supports on the characteristics of Pd/C catalysts. Carbon N. Y. 1993;31:427–435.  
Available: [https://doi.org/10.1016/0008-6223\(93\)90130-3](https://doi.org/10.1016/0008-6223(93)90130-3)
47. Tchuifon TDR, Anagho SG, Ketcha JM, Ndifor-angwafor NG, Ndi JN. Kinetics and equilibrium studies of adsorption of phenol in aqueous solution onto activated carbon prepared from rice and coffee husks. International Journal of Engineering and Technical Research. 2014;2(10):166–173.
48. Ofomaja AE. Sorptive removal of Methylene blue from aqueous solution using palm kernel fibre: Effect of fibre dose. Biochem. Eng. J. 2008;40:8–18.  
Available: <https://doi.org/10.1016/j.bej.2007.11.028>
49. Mohamed FS, Khater WA, Mostafa MR. Characterization and phenols sorptive properties of carbons activated by sulphuric acid. Chem. Eng. J. 2006;116:47–52.  
Available: <https://doi.org/10.1016/j.cej.2005.10.015>
50. Muhammad M, Ali Khan M, Choong TSY. Adsorptive separation studies of beta-carotene from methyl ester using mesoporous carbon coated monolith. J. Chem. 2012;2013.  
Available: <https://doi.org/10.1155/2013/235836>
51. Kumar A, Kumar S, Kumar S. Adsorption of resorcinol and catechol on granular activated carbon: Equilibrium and kinetics. Carbon N. Y. 2003;41:3015–3025.  
Available: [https://doi.org/10.1016/S0008-6223\(03\)00431-7](https://doi.org/10.1016/S0008-6223(03)00431-7)
52. Suresh S, Srivastava VC, Mishra IM. Isotherm, thermodynamics, desorption, and disposal study for the adsorption of catechol and resorcinol onto granular activated carbon. J. Chem. Eng. Data. 2011;56:811–818.  
Available: <https://doi.org/10.1021/je100303x>

© 2018 Patricia et al.; This is an Open Access article distributed under the terms of the Creative Commons Attribution License (<http://creativecommons.org/licenses/by/4.0>), which permits unrestricted use, distribution, and reproduction in any medium, provided the original work is properly cited.

*Peer-review history:*  
*The peer review history for this paper can be accessed here:*  
<http://www.sciencedomain.org/review-history/27684>